Electronic Effects and Ring Strain Influences on the Electron Uptake by Selenium-Containing Bonds

ÉLISE DUMONT,[1] PIERRE-FRANÇOIS LOOS,[2] ADÈLE D. LAURENT,[2] XAVIER ASSFELD[2]

[1]*Laboratoire de Chimie, UMR 5182 CNRS École Normale Supérieure de Lyon, 46 allée d'Italie, 69364 Lyon Cedex 07, France*

[2]*Équipe de Chimie et Biochimie Théoriques, UMR 7565 CNRS-UHP, Institut Jean Barriol (FR CNRS 2843), Faculté des Sciences et Techniques, Nancy-Université, B.P. 239, 54506 Vandoeuvre-lès-Nancy, France*

Received 24 November 2008; accepted 22 December 2008
Published online 16 June 2009 in Wiley InterScience (www.interscience.wiley.com).
DOI 10.1002/qua.22072

ABSTRACT: The gas-phase electron attachment of thiaselena and diselena derivatives is investigated on model organic systems by ab initio calculations (level of theory MP2/DZP++). Electronic contributions favor the one-electron addition on selenium-containing compounds, with adiabatic electron affinities of 0.03, 0.24, and 0.43 eV, respectively, for dimethyldisulfide, dimethylselenenylsulfide, and dimethyldiselenide. This ensures the possibility of an excess electron binding on —Se—S— and —Se—Se— linkages. The so-formed radical anionic intermediates present a three-electrons two-centers 2c—3e bond, whose nature is confirmed by Mulliken spin densities and NBO analysis. They are stable towards dissociation, with a low barrier evaluated between about 25–60 kJ/mol. Cyclization strongly enhances dichalcogen propensity to fix an excess electron. Adiabatic electron affinities of a series of 1,2-thiaselena-cycloalkanes and 1,2-diselena-cycloalkanes are positive and range from 0.24 to 1.30 eV. This can be traced back to the release of ring strain energy upon one-electron addition: this geometrical effect is nevertheless less marked than for disulfide analogs. Int J Quantum Chem 110: 513–523, 2010

Key words: thiaselenide; diselenides; disulfide; electron attachment; three-electrons two-centers bonds; ab initio calculations; ring strain energy

Correspondence to: É. Dumont; e-mail: elise.dumont@ens-lyon.fr

Contract grant sponsor: The Jean Barriol Institute.
Contract grant sponsor: Supercomputer resources of the Pole Scientifique de Modelisation Numerique (PSMN), ENS Lyon.

1. Introduction

Selenium versatile chemistry has raised much interest in various areas [1, 2]. There is a fundamental interest in understanding its difference with sulfur analogs, in terms of structure and reactivity (spectroscopy, stereoelectronic effects). Even simple selenium-containing derivatives still need to be properly characterized [3], for instance for their environmental aspects [4]. Selenium also plays a crucial and dual role in biology [5–8]. Although its toxicity beyond certain quantities has been early recognized, evidences for its essential role in antioxidant protection have been reported: cancer protection [9, 10], Keshan disease, etc. Selenium is most often incorporated in proteins as selenocysteine (Sec), the 21st proteinogenic amino-acid. Its redox potential is lower than cysteine and this confers to selenoproteins an enhanced reactivity by a factor of 10, 100, or even 1,000 [11]. Much research efforts currently focus on enlighting the underlying mechanisms of antioxidant protection, where electron transfers play a determinant role [12]. A recent example is MsrB1, which has a much higher efficiency towards methionine sulfoxide reduction than other classes of methionine sulfoxyde reductases [13]. Other experimental studies have considered cysteine to selenocysteine mutation to design inhibitors with more controlled properties [14].

Both experimental techniques (pulse radiolysis, synchrotron X-ray,…) and ab initio calculations have ascertained the importance of transient three-electrons two-centers intermediates in the biological systems [15–18]. They present a hemi-bond, usually denoted as X.∴Y, formed by capture of a low-lying energy electron. Motivations are twofold for characterizing such species, and special importance is given to X and Y being chalcogens as it corresponds to the biologically relevent situation.

Their structure has been in-depth explored, noticeably with topological analysis [19]. Yet, less is known concerning their reactivity, and in particular the ease by which such intermediates are formed. Far from being a prototype reaction, the one-electron addition (see Fig. 1) is involved in many biochemical redox processes involving dichalcogen bridges [20].

The variation of redox potential for a sulfur-to-selenium substitution depends among others on: (i) the propensity to fix an excess electron, (ii) the barrier for the dissociation of the transient hemi-bonded intermediate, (iii) their reactivity toward hydrogen atom, or proton addition,… The central question in this article is to gain some insights on the electron affinity of thiaselena- and diselena-linkages when compared with dithia analogs (point (i)). Respective dissociation barriers (point (ii)) of the corresponding 2c—3e bonds, for which no experimental data are available, will also be briefly commented for linear systems.

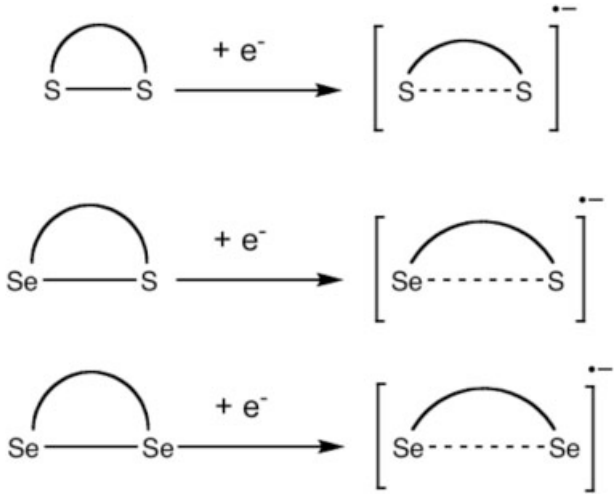

FIGURE 1. Electron attachment reaction on (a) a disulfide, (b) a selenosulfide, and (c) a diseleno bonds. The so-formed radical anions feature a three-electron two-center bond, with a drastic lengthening of the initially covalent bond. The resulting hemi-bond is represented with dashed lines.

Electron affinity is intrinsically delicate to determine either experimentally or by quantum mechanics calculations [21]. Some simple linear aliphatic or aromatic disulfides have been carefully studied [22–24] but no analog results on hemi-bonded anions involving selenium are known to the best of our knowledge. The only experimental result published so far is due to King and Illies: they reported mass spectroscopy data that "*very strongly support a two-center three-electron Se.∴Se interaction in* $[(CH_3)_2Se.\therefore Se(CH_3)_2]^+$" [25].

In this article, ab initio calculations are performed to investigate the one-electron addition on selenium-containing organic compounds. The methodological aspects for describing 2c—3e bonds are briefly recalled in Section 2. It is crucial to ensure the reliability of our calculations, especially the basis set dependence, as discussed in Section 2. The reactivity of dimethydisulfide, dimethylselenenylsulfide, and dimethyldiselenide are compared in Sub- section 3.1, to evaluate the importance of in-

TABLE 1

Adiabatic electron affinities AEA (in eV) for Me—X—Y—Me compounds, at the MP2 level of theory and for several basis sets. Values in parenthesis correspond to the dif-ference of electron affinities with respect to disulfide analog. Although absolute values are strongly basis-set dependent, the respective order of reactivity is conserved.

Basis set	6-31+G**	6-31+G**(S,Se), 6–31G*(C,H)	6-311+G**	DZP++
DMDS	−0.11	−0.14	0.02	−0.16
DMSeS	0.03 (0.14)	0.03 (0.17)	0.17 (0.15)	0.01 (0.17)
DMDSe	0.21 (0.33)	0.21 (0.35)	0.37 (0.31)	0.15 (0.31)

trinsic electronic contributions. The variation of electron affinity of these model systems upon dihedral torsion is analyzed in Subsection 3.2. It provides a first estimate of geometric effects upon dichalcogen linkages. They are further investigated in Subsection 3.3 on small-members cyclic linkages.

2. Methodological Approach

Chemical bonds with an odd number of electrons constitutes a well-documented pitfall case for Hartree–Fock and DFT methods, as well-established in the literature. We have recently summarized in a more detailed way the methodological reasons for such a failure [26], and we will here simply refer the interested reader to the original analysis [27–31]. The second-order Møller–Plesset perturbation theory (MP2 [32]) ensures a proper description of the one-electron addition on dichalcogen linkages.

(U)MP2(fc) calculations, as well as NBO analysis, were performed with the Gaussian 03 series of programs [33]. $\langle S^2 \rangle$ values were never greater than 0.77 (the exact value is 0.75), such that no spin contamination will affect our results. Adiabatic electron affinities (AEA) are defined as the difference between the total energies of the neutral and radical anion states at their respective optimized geometries. Vertical electron affinities (VEA) and vertical detachment energy (VDE) are defined as the difference between the total energies of the neutral and radical anion optimized geometries, respectively.

$$\mathrm{AEA} = E(\mathrm{neutral}) - E(\mathrm{anion}) \quad (1)$$

$$\mathrm{VEA} = E(\mathrm{neutral}) - E(\mathrm{anion}) \text{ at the optimized geometry of the neutral compound} \quad (2)$$

$$\mathrm{VDE} = E(\mathrm{neutral}) - E(\mathrm{anion}) \text{ at the optimized geomtery of the anion} \quad (3)$$

A specific and key issue is the choice of the basis set [21]. We performed auxiliary calculations on three prototype dichalcogens, at the MP2 level of theory and with four different basis sets, to assess the stability of energetic quantities. Not unexpectedly, AEAs of the neutral moities and dissociation energy (E_{disso}) of the radical anions (reported in Tables I and II) are both basis-set dependent. It lies beyond the scope of this study to explore in depth this methodological aspect, and we would lack a comparison with the exact experimental values. By

TABLE II

Dissociation energies E_{disso} (in kJ/mol) for 2c—3e Me—X$^{\cdot}$.Y—Me radical anions, at the MP2 level of theory and for several basis sets. Values in parenthesis correspond to the difference with respect to disulfide analog. Although absolute values are strongly basis-set dependent, the respective order of reactivity is conserved.

Basis set	6-31+G**	6-31+G**(S,Se), 6–31G*(C,H)	6-311+G**	DZP++
DMDS	28.4	26.6	26.4	28.4
DMSeS	27.9 (−0.5)	22.9 (−3.2)	26.0 (−0.4)	27.7 (−0.7)
DMDSe	38.1 (+9.7)	41.8 (15.2)	36.9 (+10.5)	38.1 (+9.7)

TABLE III

Energetic data for the one-electron addition on three prototype dichalcogen bonds Me—X—Y—Me with (X,Y=S,Se). Vertical electron affinities (VEA), vertical de-tachment energy (VDE) and adiabatic electron attachment energies AEA are given in eV (level of theory MP2/DZP++). Dissociation energies E_{disso} are given in kJ/mol. Geometri-cal parameters are also reported: the first line refers to the neutral (N) species, the second one to the radical anion (RA).

Compound		Geometrical parameters		Energetic parameters				
CH_3—X—Y—CH_3		d(X—Y)	∠(X—Y—C)	τ(C—X—Y—C)	VEA	AEA	VDE	E_{disso}
SS	N	2.05	101.5, 101.5	82.7	−1.32	0.03		
	RA	2.79 (0.74)	87.4, 87.4	84.3			1.61	28.4
SeS	N	2.20	98.6, 101.8	83.5	−1.08	0.24		
	RA	2.87 (0.67)	84.3, 90.3	82.7			1.61	27.7
SeSe	N	2.33	99.1, 99.1	84.7	−1.02	0.43		
	RA	2.97 (0.64)	87.0, 87.0	80.9			1.63	38.1

contrast, the important point is the remarkable stability of relative quantities with respect to the basis set, which is a necessary condition to discuss the factors influencing this reaction.

We chose here to use the DZP++ basis set, which has been proposed by Schaefer and coworkers [34]. It consists of the double-ζ *sp* contraction of Dunning [35, 36] augmented with one set of polarization and diffuse functions (*s* for hydrogen, *s* and *p* for heavy atoms). The latter are even tempered, following the suggestion of Lee and Schaefer [34] (Implicit inclusion of relativistic effects (through the use of pseudo-potentials) is not expected to be important for selenium [37]. We thus decided not to take them into account in our study). Its range of applicability is remarkably large, with for instance calculations of electron affinity of nucleobases (see [38] and references therein). Here, the main reason for choosing DZP++ is that this basis set has been calibrated for an accurate description of electron affinities of selenium-containing molecules (SeF_n [39], SeO_n [40],…). One can note that our AEA value for diethyldisulfide (DEDS) at the MP2/DZP++ level of theory is equal to the exact one (+0.10 eV [22, 41]).

3. Results and Discussion

3.1. ELECTRON CAPTURE BY PROTOTYPE DICHALCOGENS Me—X—Y—Me AND ORBITAL DIAGRAMS

We first examine the energetic difference between dithia-, thiaselena-, and diselena-linkages electron capture on prototype systems: dimethyldisulfide (DMDS), dimethylthioselenide (DMSeS), and dimethyldiselenide (DMDSe). The common notation Me—X—Y—Me will be used, with *X* and *Y* denoting either a sulfur or a selenium atom. Geometrical parameters for both neutral and anionic species are also reported in Table III, but will be discussed independently in Subsection 3.2. NBO analysis data and other related data (spin densities) for 2c—3e systems are reported in Table IV: they confirm the hemi-bonded nature of the radical an-

TABLE IV

NBO analysis for the three prototype dichalcogen bonds Me—X∴Y—Me with (X,Y=S,Se). *q* denotes the atomic charge (a.u.) and ρ the spin densities (Mulliken partition).

Compound	Atomic charge		Spin densities		Bond order	
CH_3—X—Y—CH_3	qX	qY	ρX	ρY	NBO	Wiberg
SS	−0.49	−0.49	0.53	0.53	0.46	0.48
SeS	−0.57	−0.49	0.58	0.47	0.47	0.50
SeSe	−0.56	−0.56	0.52	0.52	0.44	0.49

ions. Dissociation energies E_{disso} were computed and are all positive, which ensures the meta-stability of the 2c—3e Me—X.∴Y—Me species. The one-electron addition on disulfides is a highly localized phenomenon. Highest occupied molecular orbitals (HOMO) for DMDS, DMSeS, and DMDSe are given on Figure 2; not unexpectedly, thiaselena and diselena linkages present the same feature with chalocogen-centered electron density.

It is found that selenium strongly enhances the electron affinity. Replacing one of the two sulfur atoms by a selenium leads to an increase of AEA by about 0.20 eV. A second substitution further favors the one-electron addition by the same increment. The reactivity order of adiabatic electron affinities:

$$\mathrm{AEA(—S—S—)} < \mathrm{AEA(—Se—S—)} < \mathrm{AEA(—Se—Se—)} \quad (4)$$

is expected to be rather intrinsic in absence of other additive contributions (geometrical or electrostatic). It can be noted that vertical electron affinities follow this same tendency, both qualitatively and quantitatively (Let us note that VEA are negative, denoting that the geometrical relaxation (lengthening) is essential for the one-electron addition). Vertical detachment energies are very close for the three systems. This important difference of reactivity is purely electronic, arising solely from the chemical bond. (Let us recall that sulfur and selenium have very similar atomic electron affinities (respectively, 200 and 195 kJ/mol)).

Molecular orbital diagrams for the three different 2c—3e bonds, with only the σ(SS) and σ^*(SS) orbitals (respectively, the HOMO-2 and LUMO), are represented in Figure 3. They do not provide informations on AEA, but it is possible to partly conclude on VEA and, more interestingly, on the dissociation energy of the so-formed hemi-bonded radical anion. The latter find an elegant rationalization within the orbital theory proposed two decades ago by Gill and Radom [42]. The stability of a 2c—3e between two equivalent fragments is characterized by the energy E_{stab}, defined as the difference between twice the HOMO stabilization and once the LUMO destabilization. By expressing E_{stab} within the elementary Hückel formalism, one can derive two conditions for the existence and stability of a X.∴X hemi-bond. The latter exists if and only if the overlap S of hybridized axial sp^2 orbitals is inferior to 0.33 (positive value of E_{stab}) [42]. Furthermore, a derivation shows that its strength is optimal for $S = 0.17$.

The sp^2-sp^2 overlap between two sulfurs is equal to 0.13 (STO-3G basis, for the 2c—3e equilibrium intersulfur distance of 2.79 Å) [42], and slightly increases for selenium (d(Se—Se) = 2.97 Å) which has more diffuse valence orbitals. We found a value of 0.17 with the same basis, equal to the optimal value. It follows that: (i) VEA increases by 0.30 eV from DMDS to DMDSe and (ii) dissociation energy increases by about 10 kJ/mol for DMDSe.

The Se.∴S bond presents a slight dissymetry, that can be further quantified by our calculations, about

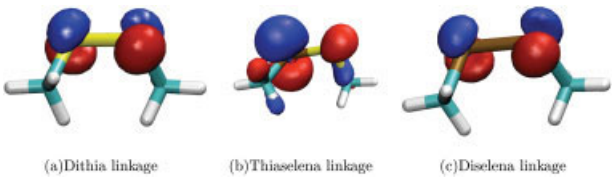

FIGURE 2. HOMO orbitals for prototypic dichalcogen linkages, for the optimized geometry at the MP2/DZP++ level of theory. Plots are drawn with the VMD package, for an isodensity of 0.06. [Color figure can be viewed in the online issue, which is available at www.interscience.wiley.com.]

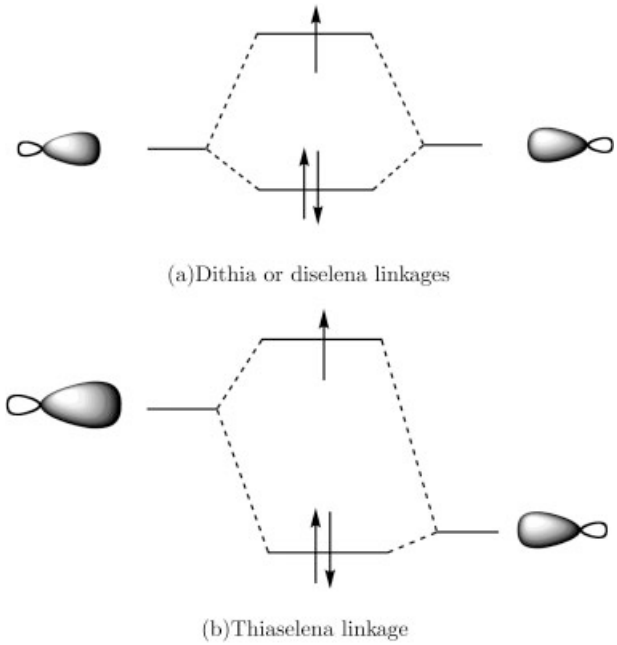

FIGURE 3. Orbitals diagrams for symmetric (a) and dissymmetric (b) dichalcogen 2c—3e hemi-bonds. The overlap S is a decisive factor governing the vertical electron affinity (VEA) and the dissociation energy E_{disso} of the radical anion.

Table IV. Atomic charges (−0.49 and −0.57 a.u. on S and Se, respectively) and spin densities (0.48 and 0.58) indicate a weak polarization, opposite to the orientation predicted with the respective atomic electronegativities. We verified that the result is similar with other basis sets.

One cannot directly conclude on the thioselenide reactivity because two antagonist contributions come into play. On the one side, the energy level difference between 3*p* and 4*p* valence orbitals of sulfur and selenium tends to weaken the 2c—3e bond [42], but, on the other side, the overlap *S* increases due to a more diffuse 4*p* valence orbital. Our calculations show that the VEA is increased by 0.24 eV, and that the resulting radical anion is associated to a slightly lower dissociation energy. The latter is a crucial quantity for understanding the outcome of the 2c—3e intermediate. Values of E_{disso} for the three hemi-bonded anions range from about 25 to 40 kJ/mol, which corresponds to the typical values for hemi-bonded systems. Selenium has a twofold orientation for E_{disso}: (i) a single substitution weakens the dichalcogen linkage by a very small amount (between 0.4 and 3.2 kJ/mol), whereas (ii) the diselena linkage is stronger and the dissociation energy increases by about 10 kJ/mol, consistently with the linear relation between *S* and E_{disso} proposed by Gill and Radom for symmetric X.∴X bonds. The following order of reactivity is found:

$$E_{\text{disso}}(-Se.\therefore S-) \approx E_{\text{disso}}(-S.\therefore S-) < E_{\text{disso}}(-Se.\therefore Se-) \quad (5)$$

which differs from the previous inequality on AEA (One can note that there is no correlation between the ease of fragmentation and the equilibrium bond lengths.) Once again, this order can be considered as rather intrinsic because of the high-local character of the one-electron addition. In fact, it might be related to some biochemical convergent observations. It is currently thought that "*selenium may facilitate reactions of protein cysteine residues by the transient formation of more reactive S-Se intermediates*" [9]. Atomic details on the underlying mechanisms are scarce: it is conjectured that selenocysteine follow a similar reactional path than cysteine, with formation of transient 2c—3e intermediates. The electron uptake is one of the rate-determining steps. At higher concentration, selenium oppositely acts as a poison; for instance, it inhibits redox-active enzymes such as thioredoxins [43]. It has been proposed that diselenides are more stable at a certain stage of the reduction process, which might be related to a less favorable dissociation of the Se.∴Se intermediate.

Molecular orbital diagrams are a powerful tool to discuss some aspects of the reactivity of selenium-containing prototype compounds (but sadly not the absolute adiabatic electron affinities). In the next subsection, we explore geometrical effects, which are expected to tune this reaction because of the drastic lengthening (by ca. 30%) concomitant to the one-electron addition. Another pieces of evidence is the well-known role of allosteric disulfides-linkages of redox-active proteins. These simple considerations have lead us to recently propose a linear relation between the topological constraint of a disulfide-linkage and its electron affinity (for both organic [26] and peptidic [44] systems). The more constrained the system, the higher its electron affinity. One of the scopes of this article is to examine the generalization to selenium-containing species. Do geometrical constraints also favor an electron uptake on selenium-contaning linkages, and, if yes, more than on disulfides?

3.2. EFFECTS OF A DIHEDRAL TORSION: ENERGETIC AND ORBITAL INTERPRETATION FOR THE ENHANCEMENT OF REACTIVITY

We focus here on the structural difference of Me—X—Y—Me compounds between (i) neutral and anionic derivatives, for a given dichalcogen linkage and, in more depth, (ii) selenium-containing molecules and their disulfide analogs. Substitution by a selenium increases the interatomic X—Y distance, by 0.15 and 0.28 Å for the neutral form and 0.08 and 0.18 Å for the radical anion. The lengthening upon one-electron uptake is of 0.73, 0.67, and 0.64 Å for the dithia, thiaselena, and diselena bonds, respectively. It is significantly weaker for selenium-containing derivatives, especially reported in relative variations (respectively, 36, 30, and 27%). One can also comment on the compression of the bending angle ∠ (C—X—Y), by about 10°; this effect can be related to the increase of the 3*p* or 4*p* character in the elongated bond, that is, the decrease of hybridization, because of the different *s* and *p* overlap [45]. The dihedral angle τ(C—X—Y—C) also exhibit important variations.

Beyond equilibrium values for distances and angles, the malleability of dichalcogen linkages is known to be important. The ease with which a dichalcogen deforms and adapts to a more rigid

aliphatic or peptidic skeleton is indeed a key feature for apprehending not only its structure, but also its reactivity. Thus, much attention has been paid to torsion profile of disulfide linkages due to their importance in atmosphere (isomerization reactions) and in biochemistry [46–48].

Disulfide electron uptake results in a threefold weakening of energetic barriers, both for the Morse curve and torsion profile [26]. Morse curves, displayed on Figure 4, indicate an immediate generalization to thiaselena- and diselena-linkages. This has a direct translation in terms of reactivity: the difference of the two curves corresponds (by definition) to the adiabatic electron affinity for a model situation where the dihedral angle τ(C—X—Y—C) is imposed. We monitor AEA along the torsion, for the three dichalcogen linkages, as displayed on Figure 5. Electron affinity is enhanced by either compression or opening of τ: corresponding increments are of 0.34, 0.26, and 0.24 eV for opening of DMDS, DMSeS, and DMDSe, respectively. For the torsion to the trans form, electron affinities are less enhanced (0.22, 0.19, and 0.20 eV, respectively). Thus, the closer inspection of numerical data reveals that DMSeS and DMDSe are intrinsically more malleable than disulfides. The damping factor that can be extrapolated from the study of model systems is 30%. As a consequence, electron affinities of selenium-containing compounds are expected to be less sensitive to geometrical constraints than their disulfide analogs.

Alternatively, one can propose a simple orbital interpretation for relative adiabatic electron affinities, on the basis of a Walsh diagram. The variation of HOMO energy π^*(SS) as a function of τ is represented on Figure 6, for DMDS. The HOMO is symmetrically destabilized by a dihedral compression ($\tau \rightarrow 0$) or opening, because of a four-electron repulsion between chalcogen lone pairs (cf. Fig. 2). One could take into account the repulsion between S—H orbitals to refine this model, and recover the dissymmetry of AEA = $f(\tau)$. Its variation can be related to the adiabatic electron affinity with the simplifying assumption that the four-electron repulsion in the radical anionic form varies much less with τ because of the drastic lengthening. The conclusion is unchanged: planar forms are more prone to fix an excess electron.

In this section, we have considered the effect of an isolated torsion on electron affinity. The dihedral angle τ is a privileged quantity, easily accessible by NMR [49], and a useful (although not perfect) indicator for predicting allosteric disulfide linkages

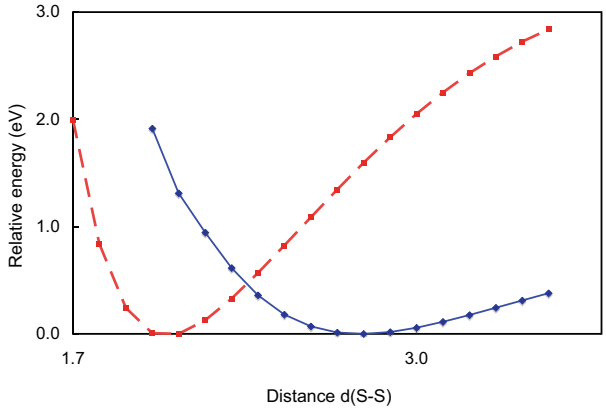

(a)Dithia linkage (DMDS)

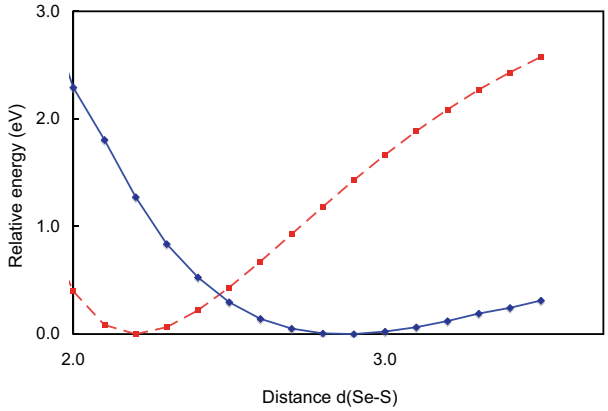

(b)Thiaselena linkage (DMSeS)

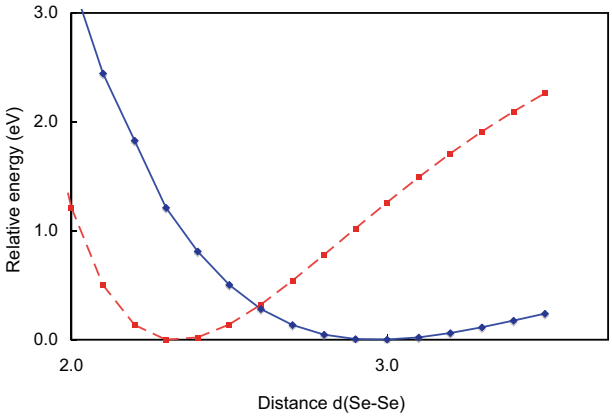

(c)Diselena linkage (DMDSe)

FIGURE 4. Morse curves for prototypical dichalcogen linkages, for neutral (dashed line) and anionic compounds (solid line). Level of theory MP2/DZP++. [Color figure can be viewed in the online issue, which is available at www.interscience.wiley.com.]

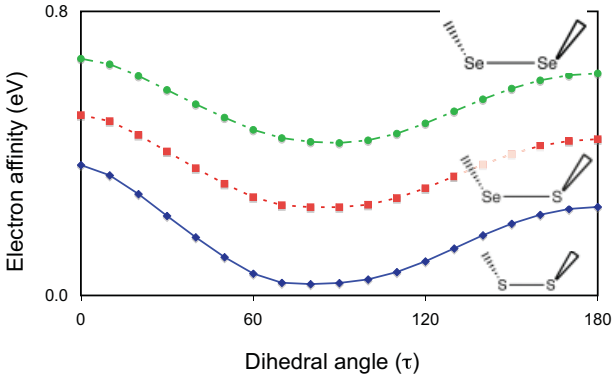

FIGURE 5. Adiabatic electron affinity (AEA, in eV) for torsional constrained prototype dichalcogens MeXYMe. Level of theory MP2/DZP++. Diamonds denote DMDS, squares DMSes, and circles DMDSe, respectively. Disulfide linkages are more sensitive to this geometrical effect: yet, electronic contributions dominate and favor electron capture by selenium-containing linkages dominate. [Color figure can be viewed in the online issue, which is available at www.interscience.wiley.com.]

[50]. Other structural parameters (bond lengths and bending angles) are also modified in cyclic compounds: the latter are studied in the next Subsection.

3.3. ELECTRON CAPTURE BY SIMPLE CYCLIC DICHALCOGENS: A LINEAR RELATION BETWEEN RING STRAIN AND ADIABATIC ELECTRON AFFINITY

We consider a series of cyclic dichalcogens (1,2-thiaselena-cycloalkanes and 1,2-diselena-cycloalkanes): the —X—Y—linkage is inserted into a more rigid aliphatic arc —$(CH_2)_n$—. Results for 1,2-dithia-cycloalkanes were analyzed in a recent paper (at the MP2/6-31+G** level of theory [26]), but are given here with the DZP++ basis set for the sake of comparison. To analyze the geometric contributions, we subtract off electronic contributions by choosing a linear aliphatic compound as a reference. It formally corresponds to the limit $n \to \infty$. We have then included three ethyl-substituted analogs Et—X—Y—Et in our set, which gives: diethyldisulfide (DEDS), diethylthioselenide (DESeS), and diethyldiselenide (DEDS). The electron affinity is enhanced (by ca. 0.10 eV) in each case for a methyl-to-ethyl substitution. It has been reported that diethyldisulfide prototypes provide a better baseline for studying the modulation of disulfide linkage electron affinity in a general way [26]. We will refer mostly to the increment:

$$\Delta AEA = AEA_{(cyclic)} - AEA_{(linear\ reference)} \qquad (6)$$

This way, we will be able to compare the ring strain effects on disulfides, thioselenides, and diselenides freely from intrinsic electronic contributions.

Structures and reactivities of the three dichalcogen linkages exhibit a very similar pattern (geometrical evolution, energetic data) with respect to cyclization. The perusal of Table V provides a more quantitative view:

1. Our calculations confirm important variations of geometric parameters, d(X—Y), ∠(X—Y—C), and τ(C—X—Y—C). The insertion of a dichalcogen, either neutral or anionic, into a small-size ring almost systematically results in an elongation of the X—Y distance, of up to about 0.10 Å (neutral $n = 2$ and anion $n = 6$) when compared with the linear reference. The sole exception is a small shortening (ca. 0.05 Å) for anionic cyclopropane derivatives ($n = 1$). We have also reported a similar "pincers" effect on disulfide-linked peptides [44].
2. Ring closure also tends to compress bending and dihedral angles. Let us note that ∠

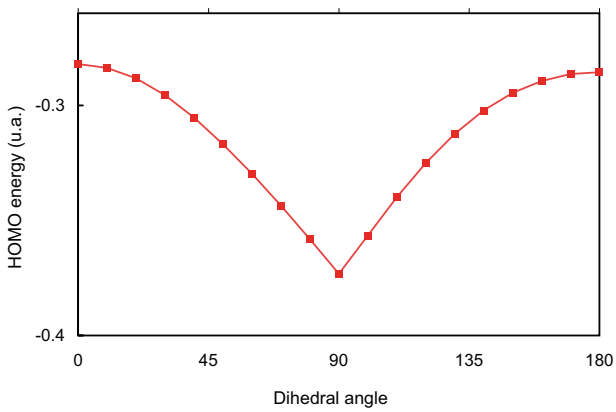

FIGURE 6. Variation of the HOMO energy for DMDS as a function of the dihedral angle τ. DMSeS and DMDSe Walsh diagramms exhibit the same pattern. It can be related in a first approximation to the adiabatic electron affinities-see text. Level of theory MP2/DZP++. [Color figure can be viewed in the online issue, which is available at www.interscience.wiley.com.]

TABLE V

Geometrical and energetical characterization of a series of aliphatic dichalcogens - neutral and associated radical anions. Calculations were performed at the MP2/DZP++ level of theory. All distances *d*(X—Y) are given in A— values in parenthesis correspond to the difference with respect to linear diethyl dichalcogen —, and angles ∠ and τ in degrees. Adiabatic electron affinities AEA are given in eV. RSE (ring strain energies) values are given in eV for neutral and radical species—see Fig. 7 for definition.

	Geometrical parameters			Energetic parameters	
X—Y bond —$(CH_2)_n$	d(X—Y)	∠(X—Y—C)	τ(C—X—Y—C)	AEA	RSE
Cyclic SS					
$n = 1$	2.10 (+0.05)	54.0	—	1.04 (+0.94)	0.90
	2.75 (−0.04)	40.4	—		n/a
$n = 2$	2.14 (+0.09)	77.9	30.5	0.98 (+0.88)	1.19
	2.85 (+0.06)	65.3	46.8		0.31
$n = 3$	2.07 (+0.02)	90.2	47.6	0.32 (+0.22)	0.38
	2.81 (+0.02)	76.3	55.9		0.16
$n = 4$	2.08 (+0.03)	98.6	46.2	0.35 (+0.25)	0.40
	2.82 (+0.03)	89.0	39.6		0.15
$n = 5$	2.05 (+0.00)	102.0	85.1	0.09 (−0.01)	0.19
	2.79 (+0.00)	93.8	83.4		0.20
$n = 6$	2.05 (+0.00)	103.1	97.6	0.10 (0.00)	0.25
	2.81 (+0.02)	94.5	100.8		0.24
DMDS					
$n \to \infty$	2.05	101.5	82.7	0.03	—
	2.79	87.4	84.3		—
DEDS					
$n \to \infty$	2.06	101.3	83.6	0.10	—
	2.79	88.6	85.3		—
Cyclic SeS					
$n = 1$	2.25 (+0.05)	49.6, 56.7	—	1.17 (+0.79)	0.79
	2.81 (−0.06)	39.5, 43.8	—		n/a
$n = 2$	2.28 (+0.08)	74.0, 78.7	21.1	1.08 (+0.70)	1.05
	2.91 (+0.04)	63.1, 67.8	25.2		0.35
$n = 3$	2.25 (+0.05)	92.1, 92.2	22.9	0.51 (+0.13)	0.31
	2.92 (+0.05)	84.0, 83.3	12.4		0.18
$n = 4$	2.24 (+0.04)	91.9, 101.5	40.6	0.54 (+0.16)	0.39
	2.89 (+0.02)	79.2, 97.2	39.4		0.23
$n = 5$	2.20 (+0.00)	101.0, 100.7	81.6	0.30 (−0.08)	0.19
	2.87 (+0.00)	95.8, 91.3	80.1		0.27
$n = 6$	2.20 (+0.00)	103.9, 102.5	72.6	0.44 (+0.06)	0.43
	2.98 (+0.12)	109.6, 101.2	44.1		0.37
DMSeS					
$n \to \infty$	2.20	98.6, 101.8	83.5	0.24	—
	2.87	84.3, 90.3	82.7		—
DESeS					
$n \to \infty$	2.20	98.5, 102.0	84.6	0.38	—
	2.87	86.1, 91.6	106.7		—
Cyclic SeSe					
$n = 1$	2.38 (+0.05)	52.3	—	1.30 (+0.78)	0.83
	2.94 (−0.03)	41.1	—		n/a
$n = 2$	2.41 (+0.08)	74.7	20.7	1.20 (+0.68)	0.97
	3.00 (+0.03)	64.7	24.4		0.30
$n = 3$	2.40 (+0.07)	91.4	25.9	0.67 (+0.15)	0.32
	3.01 (+0.04)	83.1	24.0		0.17
$n = 4$	2.37 (+0.04)	94.8	40.8	0.68 (+0.16)	0.36
	3.00 (+0.03)	86.5	38.9		0.20
$n = 5$	2.33 (+0.00)	99.2	80.3	0.47 (−0.05)	0.19
	2.97 (+0.00)	92.0	79.6		0.25
$n = 6$	2.33 (+0.00)	102.1	69.3	0.61 (+0.09)	0.44
	3.06 (+0.09)	104.5	41.0		0.35
DMDSe					
$n \to \infty$	2.33	99.1	84.7	0.43	—
	2.97	87.0	80.9		—
DEDSe					
$n \to \infty$	2.33	99.2	85.6	0.52	—
	2.97	86.5	84.0		—

(X—Y—C) tend to be smaller in radical anions by about 10°, perhaps to accomodate the drastic lengthening of the dichalcogen bond. The interpretation of this geometrical interplay is not straightforward: for instance, our calculations indicate an additional lengthening of about +0.10 Å for 1,2-thiaselena-cyclooctane and 1,2-diselena-cyclooctane ($n = 6$) rather than an angular pincement.

3. Although the structural plasticity of dichalcogen linkages leads to a fairly complicated interpretation, the modulation of AEA is more smooth. Electron affinities are strongly enhanced in cyclic compounds, although this effect rapidly attenuates with the ring size n. Clearly, the dihedral compression is not solely responsible-the curves AEA = $f(\tau)$ are not reported here because of a significant scatter. For instance, passing from DMDS to its cis conformer results in an increase of AEA of 0.34 eV, to be compared with 0.94 eV for DMDS to 1,2-dithia-cyclopropane ($n = 1$).
4. To include variations of d(X—Y) and ∠(X—Y—C) that also impact on electron affinity, it is more sounded to refer to ring strain energies (RSE), that gather all the geometrical variations. RSEs were computed according to the group equivalent method [51] (cf. Fig. 7) and are given in Table V (They could not be estimated for radical anionic derivatives of cyclopropane ($n = 1$) because the $HX^{\cdot}\therefore YCH_2X$ $\therefore YH$ dianion was found to be unstable).

- Neutral structures are most often more constrained than their radical anion. A common exception in our set is for $n = 5$: in this case, dichalcogen electron uptake is slightly less favorable than for the linear reference. Oppositely, 4-members rings ($n = 2$) are predicted to be the more reactive towards electron addition. The variation as a function of n is not monotonous.
- For cyclic systems, numerical values confirm that the more constrained the neutral dichalcogen linkage, the higher its electron affinity. We can propose a neat linear relation between ΔAEA and $RSE_{neutral}$, with the simplifying assumption that variations of RSE_{anion} can be comparatively negliged. A linear dependence is found, with R^2 regression coefficients of respectively 0.92, 0.86, and 0.91 (DMDS, DMSeS, and DMDSe, respectively). Most of the scattering observed comes from $n = 1$, probably because of the different definition of RSE.
- The slopes of AEA = $f(RSE_{neutral})$ are, respectively, 0.90, 0.84, and 0.86, which reflects a weaker sensitivity of selenium-containing linkages. Neutral cyclic compounds are significantly less strained than disulfide analogs, which is probably due to the longer interchalcogen distance.

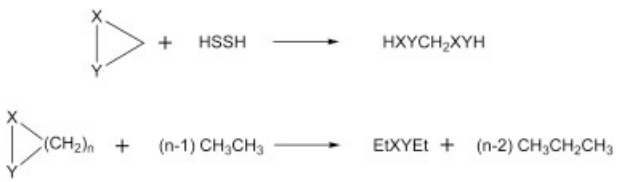

FIGURE 7. Isodesmic reactions used for the definition of ring strain energies (RSE), according to the group equivalent approach proposed by Bachrach. A specific definition is needed for cyclopropane derivatives ($n = 1$).

On the basis of this analysis of cyclic dichalcogens, a partitioning of electron affinity into two additive contributions can be proposed: an intrinsic effect arises from electronic contributions and favors thioselenide and diselenide, whereas a geometric one tends to counterbalance the order of AEAs found in Eq. (4). This could provide some first basis for predicting the preferential site of attachment of an excess electron on a disulfide-knotted motif. (Other important contributions like electrostatic ones [52] are not expected to differenciate dichalcogen linkages).

4. Concluding Remarks

In this article, we report the first ab initio calculations on the one-electron addition on thiaselena and diselena linkages. In agreement with the sole experimental result available so far on hemibonded radical cations, our calculations confirm that 2c—3e radical anions are stable towards dissociation and should be observed.

This analysis may shed lights on their role as biological intermediates, as electron addition is known to be a key step in most biochemical events [12]. Many questions concerning selenoproteins antioxydant properties are not yet elucidated. For instance, Beld et al. recently wrote: "*Surprisingly, the greater thermodynamic stability of diselenide bonds relative to disulfide*

bonds is not matched by a corresponding decrease in reactivity" [53]. This could be related to the higher dissociation energy of the hemi-bonded Se.·.Se linkage. Oppositely, the slightly weaker Se.·.S bond appears as a plausible intermediate, as conjectured in biochemistry. We plan to study the one-electron addition on seleno-containing enzymes, for which experimental informations are available.

References

1. Bachrach, S. M.; Jiang, S. J Org Chem 1999, 64, 8248.
2. Back, T. G. Encyclopedia Inorg Chem 2005, 8, 4956.
3. Trujillo, C.; Mo, O.; Yanez, M.; Silvi, B. J Chem Theor Comput 2008, 4, 1593.
4. Frankenberger, W. T.; Engberg, R. A. Environmental Chemistry of Selenium; Cambridge University Press, 1998.
5. Frost, D. V.; Lish, P. M. Ann Rev Pharm 1975, 15, 259.
6. Rederstorff, M.; Krol, A.; Lescure, A. Cell Mol Life Sci 2005, 63, 52.
7. Retey, J. Chem Biodiversity 2008, 5, 357.
8. Policar, C. Gaz Med 1995, 102, 25.
9. Ganther, H. E. Carcinogenesis 1999, 20, 1657.
10. Birringer, M.; Pilawa, S.; Flohe, L. Nat Prod Rep 2002, 19, 693.
11. Kim, H.-Y.; Gladyshev, V. S. PLos Biol 2005, 3, e375.
12. Moser, C. C.; Keske, J. M.; Warncke, K.; Farid, R. S.; Dutton, P. L. Nature 1992, 355, 796.
13. Stadtman, T. C. PLoS Biol 2005, 3, e421.
14. Armishaw, C. J.; Daly, N. L.; Nevin, S. T.; Craik, D. J.; Alewood, P. F. J Biol Chem 2006, 281, 14136.
15. Weik, M.; Bergès, J.; Raves, M. L.; Gros, P.; McSweeney, S.; Silman, I.; Sussman, J. L.; C. Houée- Levin, Ravelli, R. B. G. J Synchroton Rad 2002, 9, 342.
16. Weik, M.; Ravelli, R. B.; Silman, I.; Sussman, J. L.; Gros, P.; Kroon, J. Proc Natl Acad Sci USA 2000, 97, 623.
17. Bergés, J.; Rickards, G.; Rauk, A.; Houée-Levin, C. Chem Phys Lett 2006, 421, 63.
18. Chen, X.; Zhang, L.; Wang, Z.; Li, J.; Wans, W.; Bu, Y. J Phys Chem B 2008 (in press).
19. Fourre, I.; Silvi, B. Het Chem 2007, 18, 135.
20. Gilbert, H. F. Adv Enzymol 2006, 63, 69.
21. Rienstra-Kiracofe, J. C.; Tschumper, G. S.; Schaefer, H. F., III; Nand, S.; Ellison, G. B. Chem Rev 2002, 102, 231.
22. Carles, S.; Lecomte, F.; Schermann, J.-P. Desfrancois, C.; Xu, S.; Milles, J. M.; Bowen, K. H.; Bergès, J.; Houée-Levin, C. J Phys Chem A 2001, 105, 5622.
23. Antonello, S.; Benassi, R.; Gavioli, G.; Taddei, F.; Maran, F. J Am Chem Soc 2002, 124, 7529.
24. Antonello, S.; Daasbjerg, K.; Jensen, H.; Taddei, F.; Maran, F. J Am Chem Soc 2003, 125, 14905.
25. King, J. E.; Illies, A. J. Int J Mass Spectrosc 2003, 228, 429.
26. Dumont, E.; Loos, P.-F.; Assfeld, X. Chem Phys Lett 2008, 458, 276.
27. Braida, B.; Thogersen, L.; Wu, W.; Hiberty, P. C. J Am Chem Soc 2002, 124, 11781.
28. Gill, P. M. W.; Radom, L. J Am Chem Soc 1988, 110, 4931.
29. Clark, T. J Am Chem Soc 1988, 110, 1672.
30. Braida, B.; Hiberty, P. C.; Savin, A. J. J Phys Chem A 1998, 102, 7872.
31. Hiberty, P. C.; Humbel, S.; Danovich, D.; Shaik, S. J Am Chem Soc 1995, 117, 9003.
32. Møller, C.; Plesset, M. S. Phys Rev 1934, 46, 618.
33. Frisch, M. J.; Trucks, G. W.; Schlegel, H. B.; Scuseria, G. E.; Robb, M. A.; Cheeseman, J. R.; Montgomery, Jr., J. A.; Vreven, T.; Kudin, K. N.; Burant, J. C.; Millam, J. M.; Iyengar, S. S.; Tomasi, J.; Barone, V.; Mennucci, B.; Cossi, M.; Scalmani, G.; Rega, N.; Petersson, G. A.; Nakatsuji, H.; Hada, M.; Ehara, M.; Toyota, K.; Fukuda, R.; Hasegawa, J.; Ishida, M.; Nakajima, T.; Honda, Y.; Kitao, O.; Nakai, H.; Klene, M.; Li, X.; Knox, J. E.; Hratchian, H. P.; Cross, J. B.; Bakken, V.; Adamo, C.; Jaramillo, J.; Gomperts, R.; Stratmann, R. E.; Yazyev, O.; Austin, A. J.; Cammi, R.; Pomelli, C.; Ochterski, J. W.; Ayala, P. Y.; Morokuma, K.; Voth, G. A.; Salvador, P.; Dannenberg, J. J.; Zakrzewski, V. G.; Dapprich, S.; Daniels, A. D.; Strain, M. C.; Farkas, O.; Malick, D. K.; Rabuck, A. D.; Raghavachari, K.; Foresman, J. B.; Ortiz, J. V.; Cui, Q.; Baboul, A. G.; Clifford, S.; Cioslowski, J.; Stefanov, B. B.; Liu, G.; Liashenko, A.; Piskorz, P.; Komaromi, I.; Martin, R. L.; Fox, D. J.; Keith, T.; Al-Laham, M. A.; Peng, C. Y.; Nanayakkara, A.; Challacombe, M.; Gill, P. M. W.; Johnson, B.; Chen, W.; Wong, M. W.; Gonzalez, C.; Pople, J. A. Gaussian, Inc.: Wallingford, CT, 2004.
34. Lee, T. J.; Schaefer, H. F. J Chem Phys 1985, 83, 1784.
35. Huzinaga, S. J Chem Phys 1965, 42, 1293.
36. Dunning, T. H., Jr. J Chem Phys 1970, 53, 2823.
37. Pearson, J. K.; Boyd, R. J. J Phys Chem A 2008, 112, 1013.
38. Gu, J.; Xie, Y.; Schaefer, H. F. Nucleic Acids Res 2007, 35, 5165.
39. Li, Q.; Xu, W.; Xie, Y.; Schaefer, H. F. J Phys Chem A 1999, 103, 7496.
40. Xu, W.; Bai, W. J Mol Struct (Theochem) 2008, 863, 1.
41. Braida, B.; Hiberty, P. C. J Phys Chem A 2003, 107, 4741.
42. Gill, P. M. W.; Radom, L. J Am Chem Soc 1987, 110, 4931.
43. Gromer, S.; Johansson, L.; Bauer, H.; Arscott, L. D.; Rauch, S.; Ballou, D. P.; Williams, C. H.; Schirmer, R. H.; Arner, E. S. Proc Natl Acad Sci 2006, 100, 12618.
44. Dumont, E.; Loos, P.-F.; Assfeld, X. J Phys Chem B 2008, 112, 13661.
45. Kutzelnigg, W. Angew Chem Int Ed Eng 1984, 23, 272.
46. Maciel, G. S.; Barreto, P. R. P.; Palazzetti, F.; Lombardi, A.; Aquilanti, V. J Chem Phys 2008, 129, 164302.
47. Haworth, N. L.; Gready, J. E.; George, R. A.; Wouters, M. A. Mol Simul 2007, 33, 475.
48. Jorgensen, F. S.; Snyder, J. P. Tetrahedron 1979, 35, 1399.
49. Van Wart, H. E.; Lewis, A.; Scheraga, H. A.; Saeva, F. D. Proc Natl Acad Sci USA 1973, 70, 2619.
50. Wouters, M. A.; George, R. A.; Haworth, N. L. Curr Protein Pept Sci 2007, 8, 484.
51. Bachrach, S. M.; Woody, J. T.; Mulhearn, D. C. J Org Chem 2002, 67, 8983.
52. Dumont, E.; Loos, P.-F.; Laurent, A. D.; Assfeld, X. J Chem Theor Comput 2008, 4, 1171.
53. Beld, J.; Woycechowsky, K. J.; Hilvert, D. Biochemistry 2007, 46, 5382.